



Published in final edited form as:

*J Am Chem Soc.* 2010 September 29; 132(38): 13533–13544. doi:10.1021/ja106284s.

## Asymmetric Total Synthesis of Vindorosine, Vindoline and Key Vinblastine Analogues

Yoshikazu Sasaki<sup>†</sup>, Daisuke Kato<sup>†</sup>, and Dale L. Boger<sup>\*</sup>

Department of Chemistry and The Skaggs Institute for Chemical Biology, The Scripps Research Institute, 10550 North Torrey Pines Road, La Jolla, California 92037

### Abstract

Concise asymmetric total syntheses of vindoline (**1**) and vindorosine (**2**) are detailed based on a unique intramolecular [4+2]/[3+2] cycloaddition cascade of 1,3,4-oxadiazoles inspired by the natural product structures. A chiral substituent on the tether linking the dienophile and oxadiazole was used to control the facial selectivity of the initiating Diels–Alder reaction and set the absolute stereochemistry of the remaining six stereocenters in the cascade cycloadduct. This key reaction introduced three rings and four C–C bonds central to the pentacyclic ring system setting all six stereocenters and introducing essentially all the functionality found in the natural products in a single step. Implementation of the approach for the synthesis of **1** and **2** required the development of a ring expansion reaction to provide a 6-membered ring suitably functionalized for introduction of the  $\Delta^{6,7}$ -double bond found in the core structure of the natural products. Two unique approaches were developed that defined our use of a protected hydroxymethyl group as the substituent that controls the stereochemical course of the cycloaddition cascade. In the course of these studies, several analogues of vindoline were prepared containing deep-seated structural changes presently accessible only by total synthesis. These analogues, bearing key modifications at C6–C8, were incorporated into vinblastine analogues and used to probe the unusual importance (100-fold) and define the potential role of the vinblastine  $\Delta^{6,7}$ -double bond.

### Introduction

Vindoline (**1**),<sup>1,2</sup> a major alkaloid of *Cantharanthus roseus*, constitutes the more complex lower half of vinblastine (**4**)<sup>2–5</sup> and serves as both a biosynthetic<sup>3,4</sup> and synthetic<sup>6,7</sup> precursor to this important natural product (Figure 1). Vinblastine (**4**) and vincristine (**5**) represent the most widely recognized members of the vinca alkaloids as a result of their clinical use as antitumor drugs. Originally isolated in trace quantities from *Cantharanthus roseus* (L.) G. Don,<sup>3</sup> their biological properties were among the first to be shown to arise from inhibition of microtubule formation and mitosis that today is still regarded as one of the more successful drug targets for the treatment of cancer.<sup>3–5</sup> We previously reported the development of a concise total synthesis of (–)- and *ent*-(+)-vindoline<sup>8–10</sup> enlisting a powerful intramolecular tandem [4+2]/[3+2] cycloaddition cascade of 1,3,4-oxadiazoles with resolution of a key intermediate,<sup>11</sup> its extension to the preparation of a series of related natural products including vindorosine (**2**),<sup>10,12</sup> and the subsequent development of a biomimetic Fe(III)-promoted coupling with catharanthine (**3**) for their single step incorporation into total syntheses of vinblastine, vincristine, and related natural products.<sup>6f</sup>

boger@scripps.edu.

<sup>†</sup>These authors contributed equally to the work.

Supporting Information Available. Full experimental details and compound characterizations are provided. This material is available free of charge via the internet at <http://pubs.acs.org>.

Herein, we report full details<sup>13</sup> of the development of asymmetric total syntheses of vindoline (**1**) and the related natural product vindorosine (**2**) based on an additional implementation of the tandem [4+2]/[3+2] cycloaddition reaction in which the tether linking the initiating dienophile and oxadiazole bears a chiral substituent that sets absolute stereochemistry of the remaining six stereocenters in the cascade cycloadducts (Figure 2).

Relative to our early work,<sup>10</sup> the dienophile linking tether was reduced in length by one carbon insuring that the initiating Diels–Alder reaction could be conducted under milder conditions<sup>11</sup> than previously observed. More significantly, this change permitted the effective control of the facial selectivity of the initiating Diels–Alder reaction and subsequent transmission of the attached substituent stereochemistry throughout the newly constructed pentacyclic ring system that was not observed with a longer dienophile tether.<sup>10</sup> The approach required that the activating acyl chain carbonyl now reside in the dipolarophile tether and that the initiating Diels–Alder reaction of the cycloaddition cascade afford a fused 5-membered ring. A subsequent ring expansion to provide the unsaturated 6-membered ring found in the core structure of the natural products was anticipated to be accomplished by using a hydroxymethyl side chain substituent that, upon alcohol activation for displacement, would undergo aziridinium ion formation and subsequent nucleophilic attack to provide a more stable 6- versus 5-membered ring suitably functionalized for introduction of the  $\Delta^{6,7}$ -double bond. As detailed herein, this rearrangement is subject to stereoelectronic control for both the aziridinium ion formation as well as its subsequent cleavage by nucleophilic attack, the latter of which also proved to be subject to kinetic and thermodynamic control of the regioselectivity. Investigations into these issues provided a unique and remarkably concise approach to the total synthesis of the natural products, clarified an important stereochemical requirement for the final regioselective elimination, and ultimately led to the development of an additional second unanticipated approach to the key ring expansion.

## Results and Discussion

### Cycloaddition substrate preparation and examination of the cycloaddition cascade

The most important question addressed in initial studies was the stereochemical fate of the key cycloaddition cascade. In prior studies, we observed significant differences in the rate and facility of the reaction that was dependent on the stereochemistry of the initiating dienophile. Although both (*Z*)- and (*E*)-enol ethers proved successful at initiating the cycloaddition cascade, the reaction rate for the (*Z*)-isomer, providing directly the correct C4 stereochemistry, was considerably slower than the corresponding (*E*)-isomer, the latter of which required an inversion of the cycloadduct C4 stereochemistry for use in the targeted synthesis.<sup>10</sup> Accordingly, substrates bearing both the (*Z*)-enol ether illustrated in Figure 2 as well as the corresponding (*E*)-enol ether were prepared and examined (Scheme 1). The side chain chirality was set using aspartic acid as the starting material (both enantiomers prepared, natural enantiomer series shown). Teoc protection of D-H<sub>2</sub>N-Asp(OBn)-OH (**6**, quant.) followed by mixed anhydride formation (*i*-BuOCOCl, NMM, DME, -15 °C, 15 min) and its reduction (NaBH<sub>4</sub>, H<sub>2</sub>O, -20 °C) provided the primary alcohol **8** (91%), which was protected as its MOM ether **9** (MOMCl, *i*-Pr<sub>2</sub>NEt, CH<sub>2</sub>Cl<sub>2</sub>, 25 °C, 2 h, 84%).<sup>14</sup> Benzyl ester hydrogenolysis (H<sub>2</sub>, 10% Pd/C, THF, 25 °C, 0.5 h), coupling of the crude carboxylic acid with *N,O*-dimethylhydroxylamine (1.2 equiv EDCI, DMAP, *i*-Pr<sub>2</sub>NEt, CH<sub>2</sub>Cl<sub>2</sub>, 0–25 °C, 16 h, 94% from **9**), and reaction of the Weinreb amide **10**<sup>15,16</sup> with EtMgBr (3 equiv, 3 equiv of CeCl<sub>3</sub>, THF, 0 °C, 1 h, quant.) cleanly provided the ethyl ketone **11**. Notably, the reaction of the Grignard reagent with a substrate closely related to **10** (–OTBS vs –OMOM) in the absence of CeCl<sub>3</sub> was considerably less effective (67% vs quant.).<sup>17</sup> Wittig olefination with Ph<sub>3</sub>P=CHOBn<sup>18</sup> provided a 1:1 mixture of the separable (*E*) and (*Z*) enol ethers **12**, which were independently carried through the subsequent 3–4 steps for oxadiazole

formation and the preparation of (*E*)- and (*Z*)-**15**. Thus, their Teoc deprotection (Bu<sub>4</sub>NF) and treatment of the crude amines with carbonyldiimidazole afforded (*Z*)- and (*E*)-**13** (86–100%) that were converted to the oxadiazole precursors **14** by treatment with methyl oxalyldiazide<sup>19</sup> in the presence of HOAc. Cyclization to form the corresponding oxadiazoles **15** was mediated by TsCl and Et<sub>3</sub>N (CH<sub>2</sub>Cl<sub>2</sub>, 94–97%). Coupling of (*Z*)-**15** and (*E*)-**15** with 2-(1-methylindol-3-yl)acetic acid (**16**) provided the substrates (*Z*)-**17** and (*E*)-**17**, respectively, with which the initial examination of the cycloaddition cascade was conducted. Although they lack the aryl methoxy substituent required for the total synthesis of vindoline, they are substrates that lead to vindorosine and were judged to be ideal surrogates for detailed examination of the key cycloaddition reaction.

As detailed in early studies, trisubstitution on the dienophile typically precludes [4+2] cycloaddition initiation of the reaction cascade.<sup>11</sup> The exception to this generalization is the use of trisubstituted olefins bearing an electron-donating substituent to activate the tethered dienophile for participation in an inverse electron demand Diels–Alder reaction with the electron-deficient 1,3,4-oxadiazole. The additional shortening of the dienophile tether length from four to three atoms was expected to further enhance this reactivity leading to a cycloaddition cascade that would proceed under milder conditions than previously observed. Thus, the electron-rich dienophiles of (*Z*)-**17** and (*E*)-**17** were judged to be well suited for initiation of the cycloaddition cascade enhancing the intrinsic reactivity of the dienophile, reinforcing the [4+2] cycloaddition regioselectivity dictated by the dienophile tether, and introducing the C4 alkoxy substituent. The distinction in the two substrates is that (*Z*)-**17** permits the direct introduction of the naturally occurring C4 stereochemistry, whereas (*E*)-**17** provides the C4 isomer requiring a subsequent inversion of configuration at this center. Cyclization of (*E*)-**17** proceeded cleanly and effectively providing essentially or predominantly a single diastereomer **20** in superb conversions (72%, xylene, 145–150 °C, 10 h) and only small amounts (0–13%) of a second diastereomer were occasionally isolated (Scheme 2). Notably, the temperature needed to initiate the cycloaddition cascade is lower (145 vs 180 °C) and the reaction time required for complete reaction is shorter (10 vs 24 h) than those observed with substrates bearing a longer dienophile tether.<sup>10</sup> In fact, (*E*)-**17** possessed sufficient reactivity that cycloaddition was observed even in refluxing toluene (110 °C), albeit requiring longer reaction times (e.g., 50% **20** at 66 h). Diastereoselective reductive cleavage of the oxido bridge in **20** was effected by treatment with NaCNBH<sub>3</sub> (2 equiv, 20% HOAc/*i*-PrOH, 0–25 °C, 40 min, 94%) in a reaction that proceeds by acid-catalyzed generation of an acyliminium ion flanked by two quaternary centers that is subsequently reduced by hydride addition to the less hindered convex face, and provided **21** whose structure and stereochemistry were confirmed in a single crystal X-ray structure determination.<sup>20</sup> Following initial studies in which **20** was characterized and as we scaled up the reaction sequence, it proved most convenient to run the cycloaddition reaction and subsequent reductive oxido bridge cleavage without the intermediate purification of **20**, providing **21** directly in good overall conversions (70% for the two steps). By contrast and consistent with expectations,<sup>10</sup> the tandem cycloaddition of (*Z*)-**17** proved more challenging to implement. After considerable exploration, (*Z*)-**17** was found to provide the desired cycloadduct **18** as the major diastereomer (6–10:1 dr) when warmed in *o*-Cl<sub>2</sub>C<sub>6</sub>H<sub>4</sub> (140 °C, 20 h, 51–57%). Like substrate (*E*)-**17**, the reaction is initiated at the lower reaction temperatures (140 °C), but satisfactory conversions required more dilute reaction concentrations (0.1 mM vs 1–5 mM) to avoid competitive intermolecular reactions in the slower 1,3-dipolar cycloaddition. Because the immediate cycloadduct **18** proved somewhat unstable to the conditions of chromatographic purification, the crude product was typically subjected to reductive oxido bridge cleavage (NaCNBH<sub>3</sub>, HCl, THF/*i*-PrOH, 0 °C, 1 min, 99%) providing **19** directly in yields up to 61% for the two step conversion. In this case, the corresponding C18 methoxy *N,O*-ketal was isolated if the reaction was conducted in MeOH (vs *i*-PrOH) resulting from oxido bridge cleavage and solvent trap of the iminium ion

without reduction and more extended reaction times or higher reaction temperatures can lead to increasing amounts of MOM ether deprotection (0–10%) under the mildly acidic conditions employed.

The reaction cascade is initiated by [4+2] cycloaddition of the 1,3,4-oxadiazole with the tethered electron-rich enol ether whose reactivity and regioselectivity are matched to react with the electron-deficient oxadiazole in an inverse electron demand Diels–Alder reaction (Figure 2). Loss of N<sub>2</sub> from the initial cycloadduct provides a carbonyl ylide, which undergoes a subsequent 1,3-dipolar cycloaddition with the tethered indole.<sup>21</sup> The diene and dienophile substituents complement and reinforce the [4+2] cycloaddition regioselectivity dictated by the linking tether, the intermediate 1,3-dipole is stabilized by the complementary substitution at the dipole termini, and the intrinsic regioselectivity of the attached dipolarophile (indole) reinforces the [3+2] cycloaddition regioselectivity that is set by its linking chain. The chiral substituent on the dienophile tether effectively controls the facial selectivity of the initiating [4+2] cycloaddition reaction preferring that the protected hydroxymethyl group at C7 and the C5 ethyl group reside trans to one another on the newly formed 5-membered ring avoiding a cis pseudodiaxial-1,3-interaction on the sterically more congested concave face of the transition state leading to the initial [4+2] cycloadduct. This establishes the absolute stereochemistry at C5 which in turn is transmitted throughout the cascade cycloadduct where the remaining relative stereochemistry is controlled by a combination of the dienophile geometry (C4 and C5 stereochemistry) and an endo indole [3+2] cycloaddition sterically directed to the face opposite the newly formed 5-membered ring.<sup>10–12</sup> The minor diastereomer derived from the cycloaddition of (*E*)-**17** that was occasionally observed and isolated (>7–15:1) is derived from exo indole [3+2] cycloaddition on the face of the 1,3-dipole opposite the newly formed 5-membered ring (C2/C11 diastereomer) indicating that the facial selectivity for the initiating Diels–Alder reaction is >20:1 (detection limits), whereas the minor diastereomer isolated from the cycloaddition of (*Z*)-**17** (6–10:1) is derived from the alternative [4+2] cycloaddition facial selectivity and has the C7 protected hydroxymethyl group and C5 ethyl cis to one another. The latter minor diastereomer as well as **18** both are recovered unchanged when independently resubjected to thermal reaction conditions as pure samples (175 °C, 8 h), whereas the former pure minor diastereomer isolated from the reaction of (*E*)-**17** slowly converts to **20** (80–98%, whereas pure **20** is recovered unchanged) indicating that, in selected instances, the 1,3-dipolar cycloaddition may be thermally reversible, partitioning to the thermodynamically more stable reaction product ( $\Delta E = >4.9$  kcal/mol for **20**, MM2). Significantly, this latter observation accounts for the fact that this minor diastereomer was not always observed, having been funneled on to the thermodynamically more stable product because of the reaction conditions employed. With recognition of this unique ability to funnel this minor diastereomer into the desired diastereomer **20** under thermal conditions, the reaction conditions employed for (*E*)-**17** were adjusted to first promote the cycloaddition cascade (125–140 °C, 8 h, xylene), then warmed at a higher temperature of 175 °C (8 h) to promote the further in situ conversion of the minor diastereomer to **20** (74% overall following oxido bridge cleavage).

Although the stereochemical assignments were firmly established by X-ray analysis of various intermediates described herein including **21**,<sup>20</sup> detailed spectroscopic analysis of the cycloaddition products **18** and **20**, as well as their minor diastereomers, confirmed the assignments distinguishing the two series. The cycloadduct **18** exhibited diagnostic NOE's of C5-Et with C4-H, C6-H $\alpha$ , C7-H and C13-H and of C4-H with N1-Me placing them all on the  $\alpha$ -face of the structure, as well as between C2-H/C10-H $\beta$ , C6-H $\alpha$ /C7-H and C6-H $\beta$ /C19-H<sub>2</sub>. Its minor diastereomer, enantiomeric in structure with **18** except for the C7 stereochemistry, exhibited diagnostic NOE's of C5-Et with C4-H, C6-H $\beta$ , C19-H<sub>2</sub> and C13-H and of C4-H with N1-Me placing them all on the  $\beta$ -face of the structure, as well as

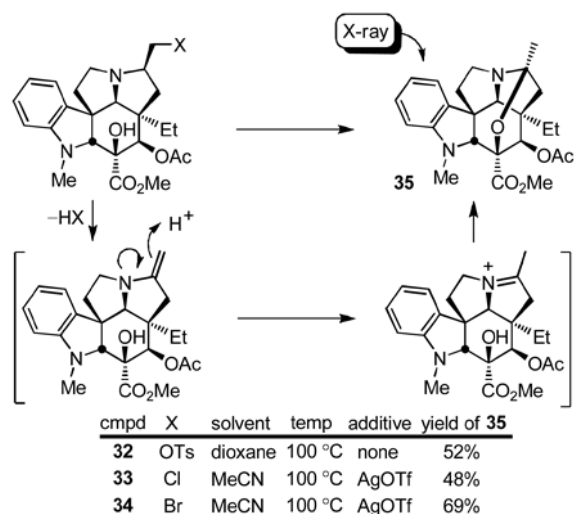
between C2-H/C10-H $\alpha$ , C6-H $\alpha$ /C7-H, and C6-H $\beta$ /C19-H<sub>2</sub>. The cycloadduct **20** exhibited diagnostic NOE's of C5-Et with C4-OBn, C6-H $\alpha$ , C7-H, and C13-H and failed to show a C4-H/N1-Me NOE. Instead, C4-H exhibited an NOE with C6-H $\beta$  and the expected NOE's of C6-H $\beta$ /C19-H<sub>2</sub> and C6-H $\alpha$ /C7-H were observed. Its minor diastereomer, epimeric only at C2 and C11, displayed diagnostic NOE's of C5-Et with C2-H and C10-H $\alpha$  and no longer displayed an NOE with C13-H. Otherwise, the diagnostic NOE's of **20** characterizing the C3–C7 stereochemistry were also observed with this minor diastereomer (C5-Et with C4-OBn, C6-H $\alpha$ , and C7-H, C4-H/C6-H $\beta$ , C6H $\beta$ /C19-H<sub>2</sub>, and C6-H $\alpha$ /C7-H).

### Asymmetric total synthesis of vindorosine

With **19** and **20** in hand, their conversion to vindorosine was explored as a prelude to efforts on vindoline itself. Vindorosine (**2**)<sup>22</sup> is among the most highly functionalized and stereochemically rich natural products within the family of alkaloids isolated from the Madagascan periwinkle (*Catharanthus roseus* (L.) G. Don). It is identical in structure to vindoline with the exception that it lacks the C16 methoxy substituent. As a consequence, it has been the subject of a series of beautiful and historically important total syntheses.<sup>10,23</sup>

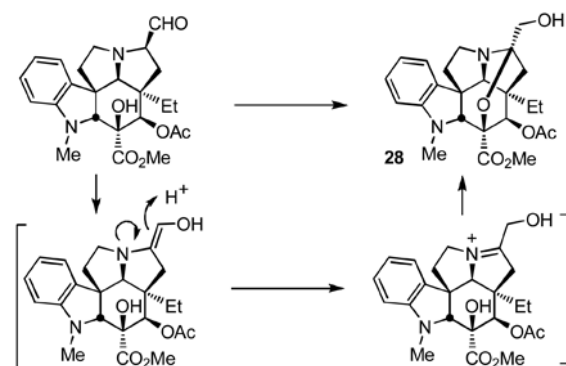
The two cycloadducts **19** and **21** were converted to the same key intermediate **24** by hydrogenolysis of benzyl ether **19** to liberate the free alcohol or benzyl ether hydrogenolysis (86%), oxidation of the free alcohol **22** to the ketone **23** (IBX, DMSO, 25 °C, 3.5 h, 78%) and diastereoselective ketone reduction (LiAl(O*t*Bu)<sub>3</sub>H, THF, 0 °C, 12 h, 90%, 10:1 dr) from the less hindered convex face for **21** (Scheme 3).<sup>24,25</sup> Subsequent C4 alcohol acetylation (Ac<sub>2</sub>O, DMAP, pyridine, 25 °C, 1 h, 98%) provided **25**. Consequently, the routes to vindorosine from either **19** or **21** converged requiring only the additional two steps of oxidation and reduction for the inversion of the C4 stereochemistry for utilization of **21**.

Several approaches for the conversion of **25** to vindorosine were examined and the first of the most concise routes that emerged from the efforts is summarized in Scheme 3.<sup>24</sup> Reductive removal of the lactam carbonyl was most directly accomplished by *O*-methylation (MeOTf, 2,6-di-*t*-butylpyridine, CH<sub>2</sub>Cl<sub>2</sub>, 25 °C, 2 h) followed by NaBH<sub>4</sub> reduction of the intermediate methoxyiminium ion (MeOH, 25 °C, 5 min, 89%) to provide **26**, although alternative approaches involving thiolactam formation and reduction also proved effective. Having liberated the basic amine and following MOM ether deprotection of **26** (HCl, MeOH, 25 °C, 4 h, 92%) to liberate the primary alcohol **27**, the ring expansion by way of alcohol activation and aziridinium ion formation was examined. Disappointingly albeit not surprising, all efforts to effect the ring expansion upon activation of the alcohol **27** by way of conversion to the tosylate **32** (TsCl, DMAP, Et<sub>3</sub>N, CH<sub>2</sub>Cl<sub>2</sub>, 25 °C, 16 h, 91%), chloride **33** (Ph<sub>3</sub>P–CCl<sub>4</sub>, Et<sub>3</sub>N, MeCN, 80 °C, 30 min, 90%), or bromide **34** (Ph<sub>3</sub>P–CBr<sub>4</sub>, Et<sub>3</sub>N, MeCN, 25 °C, 30 min, 96%) failed to lead to aziridinium ion formation (equation 1). Instead and only upon exposure to forcing conditions, such derivatives simply led to elimination and subsequent *N,O*-ketal formation to provide **35** whose structure and stereochemistry were confirmed by X-ray analysis<sup>26</sup> (equation 1). Protection of the C3 tertiary alcohol prevented the *N,O*-ketal formation, but still led to elimination and not aziridinium ion formation. Clearly, the geometrical constraints imposed by the fused 6,5,5-ring system, which place the nitrogen lone pair on the convex face of the molecule opposite the hydroxymethyl substituent, are sufficient to preclude its participation in the requisite stereoelectronically-controlled displacement reaction for aziridinium ion formation.<sup>27</sup>



(1)

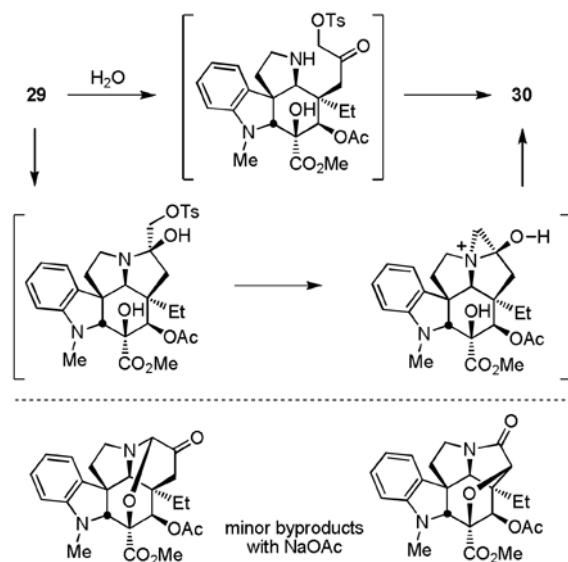
Although such an elimination reaction might be used to effect the required ring expansion and its potential was briefly examined (e.g., NBS, H<sub>2</sub>O–THF), a more attractive approach emerged as we began examining methods for the inversion of stereochemistry at C7 in order to place the hydroxymethyl substituent on the same face of the molecule as the nitrogen lone pair. Since this entails isomerization of the C7 substituent from the congested concave face of the molecule to its less hindered convex face, oxidation of the alcohol **27** to the corresponding aldehyde and its epimerization were examined. Swern oxidation (CH<sub>2</sub>Cl<sub>2</sub>, 1 h, 80%) provided an unstable  $\alpha$ -aminoaldehyde that not only rapidly epimerized, but was also especially prone to hydrate and enol formation. Moreover, we found that simply exposing the crude aldehyde to silica gel in the presence of Et<sub>3</sub>N (EtOAc) led to clean conversion to the stable *N,O*-ketal **28** (80%), equation 2.



(2)

Activation of the primary alcohol for displacement (TsCl, DMAP, Et<sub>3</sub>N, CH<sub>2</sub>Cl<sub>2</sub>, 25 °C, 16 h, 87%) followed by treatment of tosylate **29** with mild base in the presence of water (HOCO<sub>2</sub>NH<sub>4</sub>, EtOH–H<sub>2</sub>O, 50 °C, 24 h)<sup>28</sup> led to clean ring expansion to provide the 6-membered ketone **30** (76%, Scheme 2). Originally examined using NaOAc<sup>28</sup> (THF–H<sub>2</sub>O, reflux, 36 h, 65%), the conversion of **29** to **30** improved using ammonium hydrogen

carbonate (ammonium bicarbonate) and the two significant byproducts (equation 3) were no longer observed. Although several mechanistic possibilities can be envisioned for this transformation, some of which proceed through an aziridinium ion,<sup>27,28</sup> it is most simply and formally represented as hydrolysis of the *N,O*-ketal to release a reactive  $\alpha$ -tosyloxymethyl ketone followed by its intramolecular *N*-alkylation to provide the 6-membered ketone **30** (equation 3). This acyclic intermediate was not detected in the reaction mixture and could not be trapped with the inclusion of  $\text{Boc}_2\text{O}$ , but its intermediacy would nicely account for the generation of the first of the two byproducts by base-catalyzed oxidative elimination of *p*-toluenesulfenic acid to produce the corresponding aldehyde. Final conversion of **30** to vindorosine required diastereoselective reduction (L-selectride, THF,  $-78\text{ }^\circ\text{C}$ , 0.5 h, 93%)<sup>12c</sup> from the less hindered, convex face of the ketone to provide alcohol **31**, which we have previously converted to the natural product (74%)<sup>10,12</sup> enlisting a regioselective elimination reaction that occurs upon Mitsunobu activation of the secondary alcohol in the absence of added nucleophiles (Scheme 3). The approach, which was explored further with the total synthesis of vindoline, provided vindorosine in 11 or 13 steps starting from the cycloaddition precursors (*Z*)- or (*E*)-**17**, respectively.

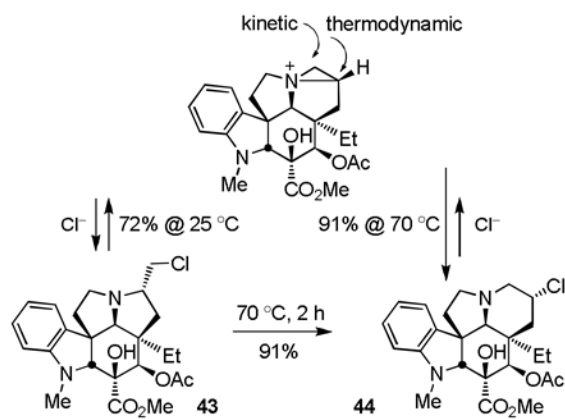


(3)

As the work progressed, we continued to pursue the use of a well-precedented ring expansion reaction proceeding via an intermediate aziridinium ion.<sup>27</sup> With the recognition that this requires inversion of the C7 stereochemistry and that a C7 aldehyde epimerization from the congested concave to convex face of the molecule is facile, we examined its potential with intermediates in which the  $\alpha$ -amino group is still a part of the adjacent amide anticipating that this would permit the generation of an intrinsically less electrophilic aldehyde (Scheme 4). Acid-catalyzed MOM deprotection of **25** (HCl,  $\text{H}_2\text{O}$ -MeOH,  $25\text{ }^\circ\text{C}$ , 7 h, 93%) and oxidation of the primary alcohol **36**<sup>29</sup> (IBX, DMSO,  $40\text{ }^\circ\text{C}$ , 3.5 h) provided the aldehyde **37** that underwent smooth and complete (>99%) epimerization to the isomeric aldehyde **38** upon exposure to silica gel (EtOAc) in the presence of  $\text{Et}_3\text{N}$  (Scheme 4). Subsequent reduction of the aldehyde **38** with  $\text{NaBH}_4$  (MeOH-THF,  $0\text{ }^\circ\text{C}$ , 0.5 h) provided the alcohol **39** (90% from **36**, 3-steps) that was reprotected as its MOM ether **40** (MOMCl, *i*-Pr<sub>2</sub>NEt,  $\text{CH}_2\text{Cl}_2$ ,  $25\text{ }^\circ\text{C}$ , 4 h, 95%). Although a bit lengthy, the first 3 steps of this sequence as well as the epimerization could be conducted without the purification or storage of

intermediates providing **39** in ca. 80% yield overall from **25** (Scheme 4). Reductive removal of the lactam carbonyl by *O*-methylation (MeOTf, CH<sub>2</sub>Cl<sub>2</sub>, 25 °C, 2 h) and NaBH<sub>4</sub> treatment of the resulting methoxyiminium ion (HCl, MeOH, 25 °C, 1 h, 70%) and subsequent MOM ether deprotection of **41** (HCl, H<sub>2</sub>O–MeOH, 25 °C, 1 h, 97%) provided the primary alcohol **42**, isomeric at C7 with the primary alcohol **27**.

Unlike **27**, activation of the primary alcohol of **42** for displacement led to aziridinium ion formation that could be kinetically trapped with nucleophiles to provide products resulting from attack on the least hindered center without ring expansion or thermodynamically trapped to provide the more stable, ring expanded products derived from attack on the more substituted center (equation 4). The latter reaction leading to ring expansion requires a nucleophile capable of reversible aziridinium ion formation and was effectively observed in reactions leading to the chlorides **43** or **44**. Thus, treatment of **42** with Ph<sub>3</sub>P–CCl<sub>4</sub> (Et<sub>3</sub>N, MeCN, 25 °C, 30 min) at room temperature provided the primary chloride **43** (72%) that on warming (MeCN, 70 °C, 2 h) smoothly converted to the ring expanded secondary chloride **44** (91%) whose structure and stereochemistry were confirmed by X-ray analysis.<sup>30</sup> Alternatively, the addition of NaI (5 equiv) to a solution containing the primary chloride **43** generated in situ at room temperature and warming the mixture at 70 °C (MeCN, 1 h) cleanly provided the ring expanded secondary iodide **45** (72–80%) whose structure and stereochemistry were also confirmed by X-ray analysis (Scheme 4).<sup>31</sup> Kuehne,<sup>32</sup> and earlier Hammer,<sup>33</sup> both describe a similar kinetic versus thermodynamic preference for aziridinium ring opening reactions, although Kuehne has also observed a reversal of this intrinsic preference<sup>32a</sup> and the propensity for even kinetic ring expansion has been generalized with simpler systems.<sup>27</sup> Interestingly and although not investigated in detail, a single effort to prepare either the corresponding primary bromide (Ph<sub>3</sub>P–CBr<sub>4</sub>) or iodide (Ph<sub>3</sub>P, I<sub>2</sub>, imidazole) from **42** provided the desired products by TLC and LCMS, but both reverted back to **42** upon aqueous workup suggesting they possess a reactivity for aziridinium ion formation that might preclude their simple isolation. Thus, the chloride addition to such an intermediate aziridinium ion is reversible, and yet sufficiently stable that it can provide two regioisomeric products whose generation is condition and temperature dependent.

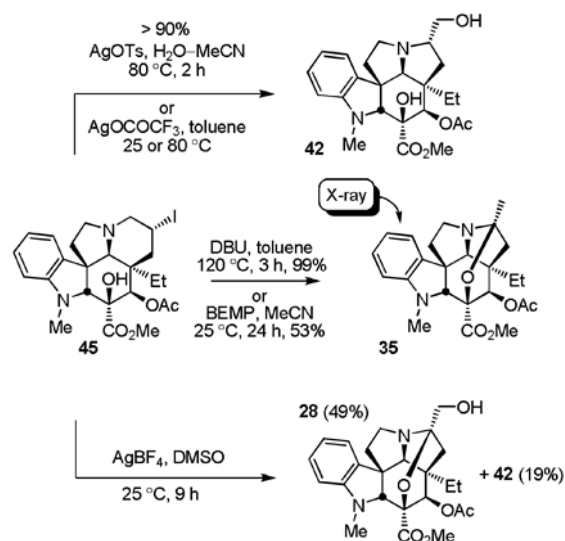


(4)

The final stages of the conversion of **44** or **45** to vindorosine also provided a series of important observations. To date, neither the chloride **44** nor the more reactive iodide **45** could be eliminated directly upon base treatment to provide vindorosine, although this was not extensively examined. Rather, and representative of the reactions observed upon use of the more forcing conditions, treatment of iodide **45** with DBU (toluene, 120 °C, 3 h)



provided **35**<sup>26</sup> (>90%, equation 5) in a reaction that apparently first undergoes ring contraction to the corresponding primary iodide, base-catalyzed elimination of HI, and subsequent *N,O*-ketal formation (see equation 1). Similarly, efforts to displace the iodide with typical oxygen nucleophiles resulted in ring contraction in reactions that also proceed through aziridinium ion formation and subsequent irreversible kinetic nucleophilic addition to its least substituted center (equation 5). An especially attractive approach combining both the ring expansion reaction with a subsequent in situ oxidation<sup>34</sup> was also initially explored at this stage and entailed the exposure of **43** or **45** to a modified Kornblum oxidation<sup>35</sup> with DMSO as the oxygen nucleophile, providing products capable of in situ oxidation to the corresponding carbonyl compound. Although treatment of **43** with AgBF<sub>4</sub>/DMSO was not productive, treatment of **45** (10 equiv AgBF<sub>4</sub>, DMSO, 25 °C, 9 h) provided **28** (49%) derived from the ring contracted aldehyde and the corresponding primary alcohol **42** (19%) indicative of kinetic DMSO addition to the less hindered carbon of the intermediate aziridinium ion followed by eliminative oxidation or solvolysis (equation 5). As highlighted and developed below, the successful implementation of this approach would require a DMSO equivalent capable of reversible aziridinium ion formation and slower in situ oxidation (elimination). Unsure whether this might be practical to implement and avoiding the complicating reactions derived from an intermediate aziridinium ion for the time being, treatment of iodide **45** with Bu<sub>3</sub>SnH in the presence of TEMPO provided the TEMPO adducts **46** (93%, 2:1 $\alpha$ : $\beta$ ) as a mixture of diastereomers (Scheme 4). Reductive cleavage of the  $\beta$ -diastereomer of the TEMPO adduct **46** (Zn, HOAc/THF/H<sub>2</sub>O 3:1:1, 60 °C, 3 h, 77%) provided the key alcohol **31** that we previously converted to vindorosine. Additionally, the isomeric C7  $\alpha$ -alcohol derived from the  $\alpha$ -diastereomer of the TEMPO adduct or the diastereomeric mixture of alcohols were oxidized to the ketone **30** (IBX, DMSO) and converted to vindorosine in two steps by diastereoselective reduction and regioselective elimination of the resulting alcohol **31** (L-selectride; Ph<sub>3</sub>P-DEAD) as detailed in Scheme 3. Significant in these studies, the additional key observation was made that efforts to eliminate a C7 leaving group bearing the  $\alpha$ -stereochemistry preferentially and nonproductively form the aziridinium ion, whereas those bearing the  $\beta$ -stereochemistry (e.g., **31**) are stereoelectronically precluded from forming an analogous aziridinium ion and productively participate in a regioselective elimination reaction to provide vindorosine.



(5)

As informative as these latter studies were, this second approach to vindorosine still suffered in length, requiring a cumbersome deprotection/reprotection/deprotection of the MOM ether in the sequence required for inversion of the hydroxymethyl side chain stereochemistry, and the final conversions to the key secondary alcohol **31** were still disappointing. Thus, after establishing the viability of the approach and following its implementation in a synthesis of vindoline, we reexamined the two limiting features of the approach. First, conditions were developed that avoid the MOM ether reprotection/deprotection of the epimerized alcohol and streamlined the preparation of the secondary iodide **45**. Thus, direct conversion of the primary alcohol **39** to the corresponding primary chloride **47** (polymer-bound Ph<sub>3</sub>P, CCl<sub>4</sub>, 25 °C, 12 h, 98%) followed by reductive removal of the lactam carbonyl (MeOTf; NaBH<sub>4</sub>) provided the sensitive primary chloride **43** avoiding the intermediate primary alcohol MOM ether protection/deprotection (Scheme 5). Direct treatment of **43**, without purification, with NaI (MeCN, 70 °C, 30 min) provided the ring expanded secondary iodide **45** in good overall conversions (59%, for 3-steps from **47**). Next, we examined modifications on the Kornblum oxidation that would permit *O*-nucleophile displacement of the iodide, albeit with the potential for reversible aziridinium ion formation with a reagent that would necessarily undergo a slower eliminative oxidation reaction to generate the ketone **30** directly. Meeting these requirements, treatment of **45** with 4-(dimethylamino)pyridine *N*-oxide (DMAPO)<sup>36</sup> under conditions that first entail aziridinium ion formation and kinetic DMAPO addition to the less substituted carbon (50 °C, 2 h, EtCN; LCMS detection of intermediate) and its subsequent partitioning to the thermodynamically more stable ring-expanded 6-membered ring addition product (120 °C, 2 h, EtCN; LCMS detection of rearrangement product), followed by treatment of the reaction mixture with base (1.5 equiv BEMP,<sup>37</sup> 25 °C, 3 h) to promote the oxidative elimination of DMAP provided the ketone **30** in a single step and in excellent conversions (78%) given the complexity of the reaction. The use of DBU<sup>36</sup> in place of BEMP was effective, but required higher reaction temperatures (80 vs 25 °C), and little or no desired product was observed without exposure of the mixture to the higher reaction temperatures (50 vs 120 °C) despite the disappearance of **45**. Efforts to convert the primary chloride **43** directly to **30** under these conditions were not as effective. However, if the conversion was conducted with KI (1.5 equiv) as an additive (3 equiv of DMAPO, 40 °C, 2 h; 120 °C, 1 h, EtCN) followed by treatment with base (3 equiv of BEMP, 25 °C, 3 h), the direct conversion of **43** to **30** was achieved in comparable overall yields (48%). Interestingly, the use of the more common and soluble NaI in place of KI simply led to unproductive and preferential consumption of DMAPO. With these modifications and following diastereoselective ketone reduction (*L*-selectride) and alcohol elimination (Ph<sub>3</sub>P-DEAD) to provide vindorosine, this second route employing a ring expansion reaction proceeding through an aziridinium ion required 12 or 14 steps from the cycloaddition substrates (*Z*)- and (*E*)-**17**, respectively,

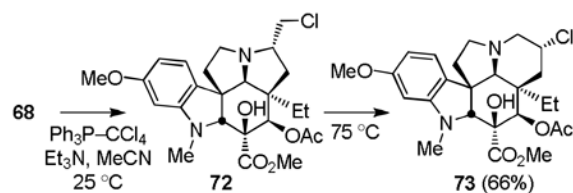
### Asymmetric total synthesis of vindoline

Coupling of both (*Z*)-**15** and (*E*)-**15** with 2-(6-methoxy-1-methylindol-3-yl)acetic acid (**48**)<sup>38</sup> provided the cycloaddition substrates (*Z*)-**49** and (*E*)-**49** for extension of the studies to the total synthesis of vindoline. Both substrates participated in the cycloaddition cascade (140 to 150 °C, 10–16 h) in a fashion analogous to **17** with the (*E*)-isomer again providing higher yields and a better diastereoselectivity than the (*Z*)-isomer (Scheme 6). In both instances, the initial cascade cycloadducts **50** and **52** were isolated and characterized, but most conveniently subjected to reductive oxido bridge cleavage prior to purification providing **51** and **53** directly, and X-ray analysis<sup>39</sup> of the primary alcohols derived from both **51** and **53** confirmed the structural and stereochemical assignments. Unlike the studies with **19** and **21**, a significant competitive indole-initiated [4+2] cycloaddition was also now observed, especially with (*Z*)-**49**, lowering the effective two-step conversions to **51** (41% vs 61% for **19**) or **53** (55% vs 70–74% for **21**).

With notable exceptions to accommodate the more nucleophilic aryl system derived from the added C16 methoxy group, most other aspects of the two approaches developed for the synthesis of vindorosine translated nicely to the synthesis of vindoline. Occasionally and with the benefit of further studies, the conversions for some steps were improved considerably. The two cycloadducts **51** and **53** were converted to the same key intermediate **56** by hydrogenolysis of benzyl ether **51** to liberate the free alcohol or benzyl ether hydrogenolysis (91%), oxidation of the free alcohol **54** to the ketone **55** (DMP, pyridine-CH<sub>2</sub>Cl<sub>2</sub> 1:4, 0 °C, 3 h, 76%) and diastereoselective ketone reduction (LiAl(O*t*Bu)<sub>3</sub>H, THF, 0 °C, 10 h, 87%) from the less hindered convex face for **53** (Scheme 7). In the conversion of **54** to **55**, IBX (vs DMP) proved less effective, and the optimized reduction of ketone **55** (87%) was established to be highly diastereoselective (30:1 dr). Subsequent C4 alcohol acetylation (Ac<sub>2</sub>O, DMAP, pyridine, 95%) provided **57**. Thus, the routes to vindoline using either **51** or **53** converged requiring only the additional two steps of oxidation (76%) and reduction (87%) for the inversion of the C4 stereochemistry for use of **53**, the product of the more effective of the cascade cycloaddition reactions.

*O*-Methylation and reductive removal of the lactam carbonyl (MeOTf, 2,6-di-*t*-butylpyridine, CH<sub>2</sub>Cl<sub>2</sub>, 25 °C, 2 h; NaBH<sub>4</sub>, MeOH, 25 °C, 5 min, 96%) followed by MOM ether deprotection (HCl, MeOH, 25 °C, 16 h) liberated the primary alcohol **59** (85% for two steps from **57**, Scheme 7). Oxidation of **59** (3 equiv of SO<sub>3</sub>-pyr, 3 equiv of Et<sub>3</sub>N, CH<sub>2</sub>Cl<sub>2</sub>-DMSO 5:1, 25 °C, 0.5 h) followed by exposure of the crude aldehyde to silica gel in the presence of Et<sub>3</sub>N (EtOAc) cleanly afforded the *N,O*-ketal **60** (85%). Formation of the primary tosylate **61** (TsCl, DMAP, Et<sub>3</sub>N, CH<sub>2</sub>Cl<sub>2</sub>, 25 °C, 16 h, 93%) and its subjection to the ring expansion reaction conditions developed herein (HOCO<sub>2</sub>NH<sub>4</sub>, EtOH-H<sub>2</sub>O, 50 °C, 24 h) provided the key 6-membered ring ketone **62** (78%) in conversions that represent an improvement over that originally reported (NaOAc, dioxane-H<sub>2</sub>O, 70 °C, 61%)<sup>13</sup>. Diastereoselective reduction of **62** (L-selectride, THF, -78 °C, 0.5 h, 91%)<sup>12c</sup> provided the penultimate secondary alcohol **63** (91%), which then underwent regioselective elimination<sup>10</sup> to provide vindoline (**1**) upon Mitsunobu activation in the absence of added nucleophiles.

In an analogous fashion and in a second route to vindoline utilizing the aziridinium ion-based ring expansion reaction (Scheme 8), MOM ether deprotection of **57** (HCl, MeOH, 25 °C, 2 h, 84%) followed by oxidation of the primary alcohol **64** to the corresponding aldehyde (1.2 equiv DMP, pyridine-CH<sub>2</sub>Cl<sub>2</sub> 1:4, 0 °C, 1 h), its clean and complete epimerization to the C7 epimeric aldehyde (SiO<sub>2</sub>, 2% Et<sub>3</sub>N-EtOAc, 25 °C), and subsequent reduction (NaBH<sub>4</sub>, MeOH-THF, 0 °C, 0.5 h) provided the C7 epimeric primary alcohol **65** (82% from **64**). MOM ether protection of **65** (98%), reductive removal of the lactam carbonyl (MeOTf, CH<sub>2</sub>Cl<sub>2</sub>, 25 °C, 2 h; NaBH<sub>4</sub>, HCl-MeOH, 0 °C, 0.5 h, 71%), and MOM ether deprotection (HCl, 85%) provided the primary alcohol **68** poised for the key ring expansion reaction. Treatment of **68** with Ph<sub>3</sub>P-CCl<sub>4</sub> for in situ generation of the primary chloride followed by addition of NaI (10 equiv) and warming the solution at 70 °C (0.5 h) provided **69** (76%) resulting from reversible aziridinium ion formation partitioning to the thermodynamically more stable secondary iodide. Finally, treatment of **69** with Bu<sub>3</sub>SnH in the presence of TEMPO followed by reduction of the TEMPO adducts **70** (Zn, HOAc, THF/H<sub>2</sub>O 2:1, 25 °C, 2 h, 78-99%) provided the penultimate secondary alcohol **63**, as well as the C7 epimeric alcohol **71**, the former of which was previously converted to vindoline (Ph<sub>3</sub>P-DEAD, THF, 25 °C, 75%). As detailed below, both **71** and **73** (equation 6) available only through implementation of this approach, as well **63**, were incorporated into vinblastine analogues.



(6)

The final improvement on this approach is detailed in Scheme 9 and follows advancements first developed with vindorosine altering the order of the steps to avoid the primary alcohol deprotection/reprotection and implementing the unique ring expansion–Kornblum oxidation. Thus, following inversion of the C7 stereochemistry, conversion of the primary alcohol **65** to the primary chloride **74** (91%) and reductive removal of the lactam carbonyl provided the chloride **72** that was immediately subjected to ring expansion treatment with NaI to provide **69** (69% from **74**). Modified Kornblum oxidation of **69** under conditions that lead to aziridinium ion formation and that thermally partition the initially formed aminooxonium addition product on to the thermodynamically more stable 6-membered ring adduct provided the ketone **62** (66%) that was previously converted to vindoline.

### Key vinblastine analogues

One of the most surprising observations made in studies with an initial series of key analogues of vinblastine<sup>6f</sup> was the impact of removing the 6,7-double bond in the vindoline subunit. The compound  $\Delta^{6,7}$ -dihydrovinblastine was found to be ca. 100-fold less active (cytotoxic) than vinblastine indicating that this region of the natural product has a pronounced impact on its properties. An examination of the recent X-ray crystal structure of vinblastine bound to tubulin<sup>40</sup> does not reveal an obvious pronounced stabilizing interaction with the olefin that might account for the difference. As a result, this impact potentially could be derived from either steric or conformational features resulting from the presence of the double bond, or arises from an effect that the olefin might have on the  $pK_a$  of the allylic amine in **1**. Several key vindoline analogues prepared herein contain subtle (**63**, **71**, and **73**) or more deep-seated changes (**59** and **68**) in this C6–C8 region of vindoline with which we could now probe the origin of this effect. Each contains a heteroatom  $\beta$  to the basic amine modulating its  $pK_a$  in a manner potentially analogous to the 6,7-double bond, and **59** and **68** incorporate the additional deep-seated change of replacing the olefin-containing 6-membered ring with a saturated 5-membered ring bearing either an  $\alpha$  or  $\beta$  oriented C7 hydroxymethyl substituent. These five compounds were coupled with catharanthine (**3**) using the single-step biomimetic Fe(III)-promoted coupling and subsequent free radical oxidation<sup>6f</sup> to afford the corresponding vinblastine analogues without optimization (Scheme 10). In addition to providing the vinblastine analogues shown, the corresponding epimeric C20' leurosidine analogues (**76**, **79**, **82**, and **85**) were generated in the now characteristic ca. 2:1  $\beta$ : $\alpha$  diastereoselectivity for the introduction of the C20' alcohol and the intermediate anhydrovinblastines (**77**, **80**, **83**, **86**, and **89**) were also isolated in yields ranging from 17–22%. Interestingly and for presently unknown reasons, the couplings and in situ oxidation of the analogues **59** and **68** containing the ring contracted 5-membered rings did not proceed nearly as well as typical substrates.

The vinblastine analogues bearing the key changes in the structure of **1** were used to further assess the importance and potential role of the 6,7-double bond in the cellular activity of the natural product (cytotoxic activity against L1210 murine leukemia and HCT116 colon cancer cell lines). Additionally, the analogues were examined for their susceptibility to

multidrug resistance (MDR), resulting from overexpression and drug efflux by Pgp, using a well-established companion vinblastine resistant cell line (HCT116/VM46).<sup>41</sup> Key elements of the results of these studies are summarized in Figure 4.

As observed in prior studies, the vinblastine analogues proved more active than the corresponding anhydrovinblastine analogues (ca 10-fold), which in turn were more active than the corresponding leurosidine derivatives (not shown, see Supporting Information). Although the vinblastine analogues containing the vindoline saturated and C7 substituted 6-membered rings (**75**, **78**, and **81**) were found to approach the activity of  $\Delta^{6,7}$ -dihydrovinblastine (**90**),<sup>42</sup> they remained at least 100-fold less potent than vinblastine. Thus, the C7 substitutions in **75** and **81** did not significantly affect the activity adversely relative to **90**, but they also did not make up for the loss in activity observed with removal of the 6,7-double bond, whereas **78** experienced a further 10-fold loss in activity. Notably, analogue **81** possesses the opportunity to generate an aziridinium ion capable of reacting with tubulin, yet its cellular activity did not reflect an enhancement in activity that would be expected to accompany such an alkylation. Finally, the vinblastine analogues **84** and **87** incorporating the vindoline subunits containing the 5-membered rings bearing a hydroxymethyl substituent were even 10-fold less potent and ca. 1000-fold less active than vinblastine. Clearly, the C6–C8 region of vinblastine including its 6,7-double bond has a surprisingly large impact on the properties of **1**, and plays a previously unappreciated major role in establishing its functional activity. Additional studies further probing this effect are in progress and will be disclosed in due time.<sup>43</sup>

## Conclusions

Full details of the development of two concise asymmetric total syntheses of vindorosine and vindoline are disclosed enlisting an intramolecular [4+2]/[3+2] cycloaddition cascade of 1,3,4-oxadiazoles in which a chiral substituent on the tether linking the dienophile and oxadiazole was used to control the facial selectivity of the initiating Diels–Alder reaction and set the absolute stereochemistry of the remaining six stereocenters in the cascade cycloadduct. Implementation of the approach for the synthesis of **1** and **2** required that the initiating Diels–Alder reaction of the cycloaddition cascade afford a fused 5-membered ring and the development of a subsequent ring expansion reaction to provide a 6-membered ring suitably functionalized for introduction of the 6,7-double bond found in the core structure of the natural products. Two unique approaches were developed for the key ring expansion that defined our use of a protected hydroxymethyl group as the substituent used to control the stereochemical course of the cycloaddition cascade. In the course of these studies, several analogues of vindoline were prepared containing deep-seated structural changes presently accessible only by total synthesis. These analogues, bearing key modifications at C6–C8, were incorporated into vinblastine analogues and used to probe the importance (100-fold) and further define the potential role of the vinblastine 6,7-double bond.

## Supplementary Material

Refer to Web version on PubMed Central for supplementary material.

## Acknowledgments

We gratefully acknowledge the financial support of the National Institutes of Health (CA042056 and CA115526) and the Skaggs Institute for Chemical Biology. We wish to thank Dr. Raj Chadha for the X-ray structures disclosed herein, William M. Robertson for the cytotoxic assays, and we are especially grateful to Dr. Paul Hellier of Pierre Fabre for the generous gift of catharanthine. D.K. is a Skaggs Fellow. Dedicated to Professor Raymond Funk in honor of his sixtieth birthday.

## References

1. Gorman M, Neuss N, Biemann K. *J Am Chem Soc.* 1962; 84:1058.
2. Moncrief JW, Lipscomb WN. *J Am Chem Soc.* 1965; 84:4963. [PubMed: 5844471]
3. (a) Noble RL, Beer CT, Cutts JH. *Ann N Y Acad Sci.* 1958; 76:882. [PubMed: 13627916] (b) Noble RL. *Lloydia.* 1964; 27:280. (c) Svoboda GH, Nuess N, Gorman M. *J Am Pharm Assoc Sci Ed.* 1959; 48:659. For related, naturally occurring vinca alkaloids: see Leurosidine: (d) Svoboda GH. *Lloydia.* 1961; 24:173. Deoxyvinblastine: (e) De Bruyn A, Sleechecker J, De Jonghe JP, Hannart J. *Bull Soc Chim Belg.* 1983; 92:485. Neuss N, Gorman M, Cone NJ, Huckstep LL. *Tetrahedron Lett.* 1968:783. N-Desmethylvinblastine: (f) Simonds R, De Bruyn A, De Taeye L, Verzele M, De Pauw C. *Planta Med.* 1984; 50:274. [PubMed: 17340313] Desacetoxyvinblastine: (g) Neuss N, Barnes AJ Jr, Huckstep LL. *Experientia.* 1975; 31:18. [PubMed: 1116520] Desacetylvinblastine: (h) Svoboda GH, Barnes AJ Jr. *J Pharm Sci.* 1964; 53:1227. [PubMed: 14249445] Anhydrovinblastine: (i) Goodbody AE, Watson CD, Chapple CCS, Vukovic J, Misawa M. *Phytochem.* 1988; 27:1713.
4. Review: Neuss, N.; Neuss, MN. *The Alkaloids.* Brossi, A.; Suffness, M., editors. Vol. 37. Academic; San Diego: 1990. p. 229
5. Reviews: (a) Pearce, HL. *The Alkaloids.* Brossi, A.; Suffness, M., editors. Vol. 37. Academic; San Diego: 1990. p. 145 (b) Borman, LS.; Kuehne, ME. *The Alkaloids.* Brossi, A.; Suffness, M., editors. Vol. 37. Academic; San Diego: 1990. p. 133
6. (a) Mangeney P, Andriamialisoa RZ, Langlois N, Langlois Y, Potier P. *J Am Chem Soc.* 1979; 101:2243. (b) Kutney JP, Choi LSL, Nakano J, Tsukamoto H, McHugh M, Boulet CA. *Heterocycles.* 1988; 27:1845. (c) Kuehne ME, Matson PA, Bornmann WG. *J Org Chem.* 1991; 56:513. Bornmann WG, Kuehne ME. *J Org Chem.* 1992; 57:1752. Kuehne ME, Zebovitz TC, Bornmann WG, Marko I. *J Org Chem.* 1987; 52:4340. (d) Magnus P, Mendoza JS, Stamford A, Ladlow M, Willis P. *J Am Chem Soc.* 1992; 114:10232. (e) Yokoshima S, Ueda T, Kobayashi S, Sato A, Kuboyama T, Tokuyama H, Fukuyama T. *J Am Chem Soc.* 2002; 124:2137. [PubMed: 11878966] Kuboyama T, Yokoshima S, Tokuyama H, Fukuyama T. *Proc Natl Acad Sci USA.* 2004; 101:11966. [PubMed: 15141084] (f) Ishikawa H, Colby DA, Boger DL. *J Am Chem Soc.* 2008; 130:420. [PubMed: 18081297] Ishikawa H, Colby DA, Seto S, Va P, Tam A, Kakei H, Rayl TJ, Hwang I, Boger DL. *J Am Chem Soc.* 2009; 131:4904. [PubMed: 19292450]
7. Review: Kuehne, ME.; Marko, I. *The Alkaloids.* Brossi, A.; Suffness, M., editors. Vol. 37. Academic; San Diego: 1990. p. 77
8. Racemic total syntheses: (a) Ando M, Büchi G, Ohnuma T. *J Am Chem Soc.* 1975; 97:6880. (b) Kutney JP, Bunzli-Trepp U, Chan KK, De Souza JP, Fujise Y, Honda T, Katsube J, Klein FK, Leutwiler A, Morehead S, Rohr M, Worth BR. *J Am Chem Soc.* 1978; 100:4220. (c) Andriamialisoa RZ, Langlois N, Langlois Y. *J Org Chem.* 1985; 50:961. (d) Ban Y, Sekine Y, Oishi T. *Tetrahedron Lett.* 1978; 2:151. (e) Takano S, Shishido K, Sato M, Yuta K, Ogasawara K. *J Chem Soc, Chem Commun.* 1978:943. Takano S, Shishido K, Matsuzaka J, Sato M, Ogasawara K. *Heterocycles.* 1979; 13:307. (f) Danieli B, Lesma G, Palmisano G, Riva R. *J Chem Soc, Chem Commun.* 1984:909. Danieli B, Lesma G, Palmisano G, Riva R. *J Chem Soc, Perkin Trans.* 1987; 1:155. (g) Zhou S, Bommeziijn S, Murphy JA. *Org Lett.* 2002; 4:443. [PubMed: 11820900]
9. Enantioselective total syntheses: (a) Feldman PL, Rapoport H. *J Am Chem Soc.* 1987; 109:1603. (b) Kuehne ME, Podhorez DE, Mulamba T, Bornmann WG. *J Org Chem.* 1987; 52:347. (c) Cardwell K, Hewitt B, Ladlow M, Magnus P. *J Am Chem Soc.* 1988; 110:2242. (d) Kobayashi S, Ueda T, Fukuyama T. *Synlett.* 2000:883.
10. (a) Ishikawa H, Elliott GI, Velcicky J, Choi Y, Boger DL. *J Am Chem Soc.* 2006; 128:10596. [PubMed: 16895428] (b) Choi Y, Ishikawa H, Velcicky J, Elliott GI, Miller MM, Boger DL. *Org Lett.* 2005; 7:4539. [PubMed: 16178578]
11. (a) Wilkie GD, Elliott GI, Blagg BSJ, Wolkenberg SE, Soenen DB, Miller MM, Pollack S, Boger DL. *J Am Chem Soc.* 2002; 124:11292. [PubMed: 12236743] (b) Elliott GI, Fuchs JR, Blagg BSJ, Ishikawa H, Tao H, Yuan Z, Boger DL. *J Am Chem Soc.* 2006; 128:10589. [PubMed: 16895427] For reviews of heterocyclic azadiene cycloaddition reactions, see: (c) Boger DL. *Tetrahedron.* 1983; 39:2869. (d) Boger DL. *Chem Rev.* 1986; 86:781. (e) Boger, DL.; Weinreb, SM. *Hetero Diels–Alder Methodology in Organic Synthesis.* Academic; San Diego: 1987.

12. (a) Elliott GI, Velcicky J, Ishikawa H, Li Y, Boger DL. *Angew Chem Int Ed.* 2006; 45:620. (b) Yuan Z, Ishikawa H, Boger DL. *Org Lett.* 2005; 7:741. [PubMed: 15704939] (c) Ishikawa H, Boger DL. *Heterocycles.* 2007; 72:95. (d) Campbell EL, Zuhl AM, Liu CM, Boger DL. *J Am Chem Soc.* 2010; 132:3009. [PubMed: 20148585] (e) Va P, Campbell EL, Robertson WM, Boger DL. *J Am Chem Soc.* 2010; 132:8489. [PubMed: 20518465]
13. Kato D, Sasaki Y, Boger DL. *J Am Chem Soc.* 2010; 132:3685. [PubMed: 20187641]
14. Rodriguez M, Llinares M, Doulut S, Heitz A, Martinez J. *Tetrahedron Lett.* 1991; 32:923.
15. Nahm S, Weinreb SM. *Tetrahedron Lett.* 1981; 22:3815.
16. Compound **10** was also prepared in a single operation (47%) from L-TeoCHN-Ser(OMOM)-OH by treatment with (1) *i*-BuOCOCl, Et<sub>3</sub>N, THF; (2) CH<sub>2</sub>N<sub>2</sub>, THF; (3) PhCO<sub>2</sub>Ag, MeNH(OMe), Et<sub>3</sub>N, THF. This avoids the use of an unnatural amino acid precursor for the natural enantiomer series.
17. Imamoto T, Takiyama N, Nakamura K, Hatajima T, Kamiya Y. *J Am Chem Soc.* 1989; 111:4392.
18. Tam TF, Fraser-Reid B. *J Chem Soc, Chem Commun.* 1980:556.
19. Christl M, Lanzendoerfer U, Groetsch MM, Ditterich E, Hegmann J. *Chem Ber.* 1990; 123:2031.
20. The structure and stereochemistry of **21** were established by X-ray (CCDC 758511) and conducted on the unnatural enantiomer series.
21. Padwa A, Price AT. *J Org Chem.* 1998; 63:556. [PubMed: 11672045] 1995; 60:6258.
22. Mosa BK, Trojaneck J. *Collect Czech Chem Commun.* 1963; 28:1427.
23. (a) Buchi G, Matsumoto KE, Nishimura H. *J Am Chem Soc.* 1971; 93:3299. [PubMed: 5559600] (b) Kuehne ME, Podhorez DE, Mulamba T, Bornmann WG. *J Org Chem.* 1987; 52:347. (c) Elliott GI, Velcicky J, Ishikawa H, Li Y, Boger DL. *Angew Chem Int Ed.* 2006; 45:620. Formal syntheses: (d) Takano S, Shishido K, Sato M, Ogasawara K. *Heterocycles.* 1977; 6:1699. (e) Veenstra SJ, Speckamp WN. *J Am Chem Soc.* 1981; 103:1645. (f) Natsume M, Utsunomiya I. *Chem Pharm Bull.* 1984; 32:2477. (g) Andriamialisoa RZ, Langlois N, Langlois Y. *J Org Chem.* 1985; 50:961. (h) Winkler JD, Scott RD, Williard PG. *J Am Chem Soc.* 1990; 112:8971. (i) Heurenx N, Wouters J, Marko IE. *Org Lett.* 2005; 7:5245. [PubMed: 16268549]
24. Often times the work was conducted with only the natural or unnatural enantiomer series (see Supporting Information), but this is represented herein depicting only the natural enantiomer series for the sake of clarity.
25. Reduction of **23** with NaBH<sub>4</sub> predominately provided the epimeric C4 alcohol **22**.
26. The structure and stereochemistry of **35** (CCDC 780504) were confirmed by X-ray analysis conducted in the unnatural enantiomer series.
27. Cossey J, Pardo DG. *Chemtracts: Org Chem.* 2002; 15:579.
28. (a) Frehel D, Badorc A, Pereillo JM, Maffrand JM. *J Heterocyclic Chem.* 1985; 22:1011. (b) Kavadias G, Velkof S, Belleau B. *Can J Chem.* 1979; 57:1861, 1866. (c) Takeda M, Inoue H, Konda M, Saito S, Kugita H. *J Org Chem.* 1972; 37:2677. (d) Hoffman RV, Jankowski BC, Carr CS, Duesler EN. *J Org Chem.* 1986; 51:130.
29. The structure and stereochemistry of **36** (CCDC 759386) were confirmed by X-ray analysis conducted in the unnatural enantiomer series.
30. The structure and stereochemistry of **44** (CCDC 759385) were confirmed by X-ray analysis conducted in the unnatural enantiomer series.
31. The structure and stereochemistry of **45** (CCDC 759387) were confirmed by X-ray analysis conducted in the natural enantiomer series.
32. (a) Kuehne ME, Okuniewicz FJ, Kirkemo CL, Bohnert JC. *J Org Chem.* 1982; 47:1335. (b) Kuehne ME, Podhorez DE. *J Org Chem.* 1985; 50:924.
33. Hammer CF, Heller SR, Craig JH. *Tetrahedron Lett.* 1972; 28:239.
34. D'hooghe M, Baele J, Contreras J, Boelens M, De Kimpe N. *Tetrahedron Lett.* 2008; 49:6039.
35. Kornblum N, Jones WJ, Anderson GJ. *J Am Chem Soc.* 1959; 81:4113. Ganem B, Boeckman RK Jr. *Tetrahedron Lett.* 1974; 15:917. Lemal DM, Fry AJ. *J Org Chem.* 1964; 29:1673. Dave P, Byun HS, Engel R. *Synth Commun.* 1986; 16:1343.
36. Mukaiyama S, Inanaga J, Yamaguchi M. *Bull Chem Soc Jpn.* 1981; 54:2221.
37. Schwesinger R. *Chimia.* 1985; 39:269.

38. Feldman PL, Rapoport H. *Synthesis*. 1986;735. Drost KJ, Jones RJ, Cava MP. *J Org Chem*. 1989; 54:5985.
39. The structure and stereochemistry of **53** were confirmed by X-ray analysis conducted the free alcohol derived by MOM ether deprotection (HCl, MeOH, 0–25 °C, 1.5 h, 66%) in the natural enantiomer series (CCDC 758510). Similarly, the structure and stereochemistry of **51** were confirmed by X-ray analysis conducted the free alcohol derived by MOM ether deprotection (HCl, MeOH, 25 °C, 16 h, quant.) in the natural enantiomer series (CCDC 780505).
40. Gigant B, Wang C, Ravelli RBG, Roussi F, Steinmetz MO, Curmi PA, Sobel A, Knossow M. *Nature*. 2005; 435:519. [PubMed: 15917812]
41. (a) Dumontet C, Sikic BI. *J Clin Oncol*. 1999; 17:1061. [PubMed: 10071301] (b) Kavallaris M, Verrills NM, Hill BT. *Drug Res Updates*. 2001; 4:392.
42. For an earlier characterization of **90**, see: (a) Neuss N, Barnes AJ, Huckstep LL. *Experientia*. 1975; 31:18. [PubMed: 1116520] (b) Barnett CJ, Cullinan GJ, Gerzon K, Hoying RC, Jones WE, Nevlon WM, Poore GA, Robison RL, Sweeney MJ, Todd GC, Dyke RW, Nelson RL. *J Med Chem*. 1978; 21:88. [PubMed: 412968]
43. Abbreviations: Ac = acetyl; BEMP = 2-*tert*-butylimino-2-diethylamino-1,3-dimethylperhydro-1,3,2-diazaphosphorine; Boc = *tert*-butoxycarbonyl; Bn = benzyl; CDI = 1,1'-carbonyldiimidazole; DBU = 1,8-diazabicyclo[5.4.0]undec-7-ene; DEAD = diethyl azodicarboxylate; DMAP = 4-(dimethylamino)pyridine; DMAPO = 4-(dimethylamino)pyridine *N*-oxide; DME = dimethoxyethane; DMF = *N,N*-dimethylformamide; DMP = Dess–Martin periodinane; DMSO = dimethylsulfoxide; EDCI = 1-[3-(dimethylamino)propyl]-3-ethylcarbodiimide hydrochloride; Fe<sub>2</sub>(ox)<sub>3</sub> = iron(III) oxalate; IBX = 2-iodoxybenzoic acid; KHMDs = potassium bis(trimethylsilyl)amide; MOM = methoxymethyl; NBS = *N*-bromosuccinimide; Pyr = pyridine; NMM = *N*-methylmorpholine; TEMPO = 2,2,6,6-tetramethylpiperidine-1-oxyl; Teoc = 2-(trimethylsilyl)ethoxycarbonyl; Teoc–O S u = 1-[2-(trimethyl-silyl)ethoxycarbonyloxy]pyrrolidin-2,5-dione; THF = tetrahydrofuran; Tf = trifluoromethanesulfonyl; Ts = *p*-toluenesulfonyl.



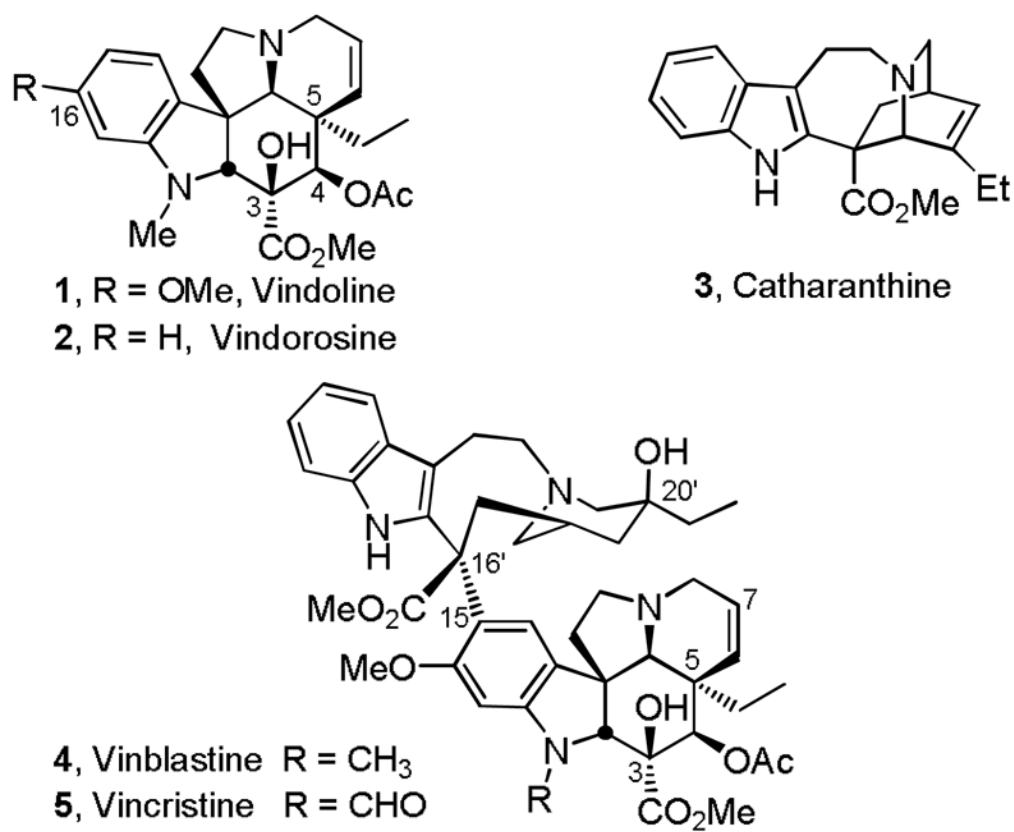


**Figure 1.**  
Natural product structures.

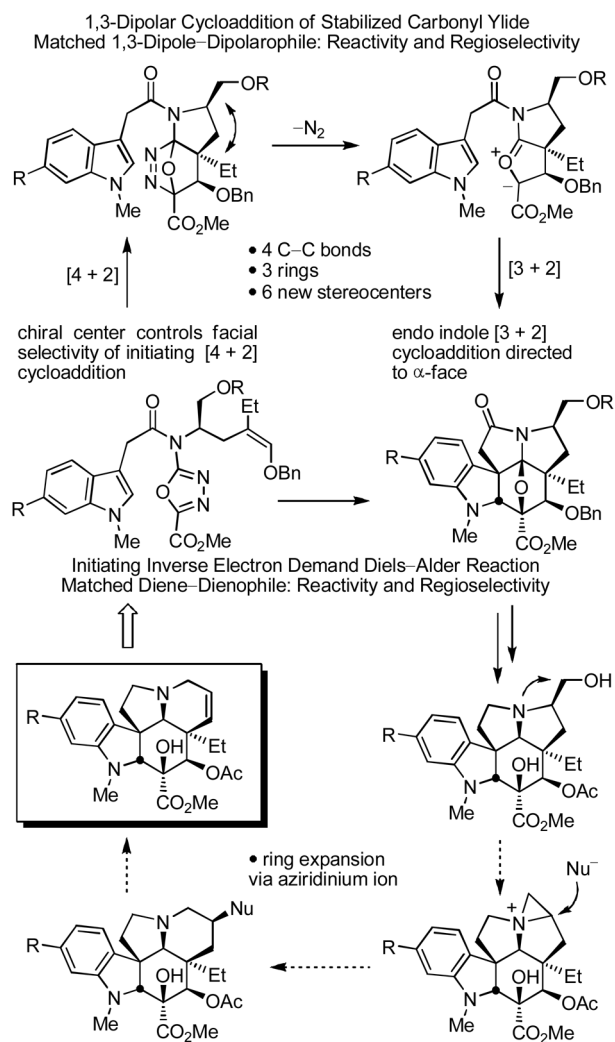
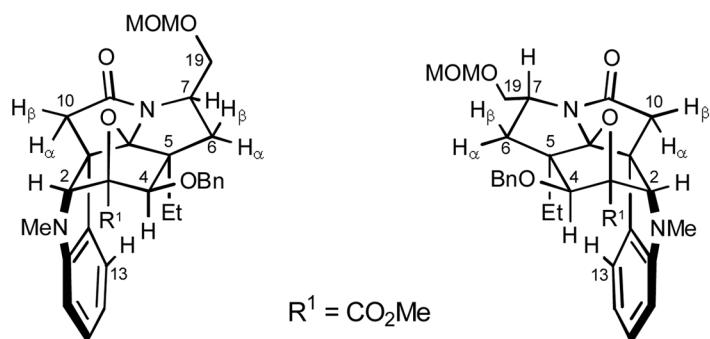
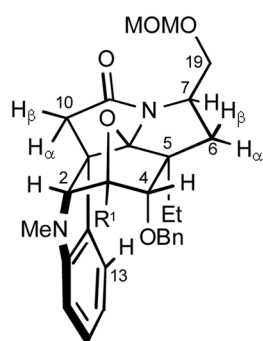


**Figure 2.**  
Key elements of the initial synthetic strategy.



**Diagnostic NOEs of **18****  
 C5-Et/ C4-H, C6-H $\alpha$ , C7-H, C13-H  
 C4-H/ N1-Me, C2-H/ C10-H $\beta$   
 C6-H $\alpha$ / C7-H, C6-H $\beta$ / C19-H $_2$

**Diagnostic NOEs for diastereomer of **18****  
 C5-Et/ C4-H, C6-H $\alpha$ , C19-H $_2$ , C13-H  
 C4-H/ N1-Me, C2-H/ C10-H $\beta$   
 C6-H $\beta$ / C7-H, C6-H $\alpha$ / C19-H $_2$



**Diagnostic NOEs of **20****  
 C5-Et/ C4-OBn, C6-H $\alpha$ , C7-H, C13-H  
 C4-H/ C6-H $\beta$ , C6-H $\beta$ / C19-H $_2$   
 C6-H $\alpha$ / C7-H

**Diagnostic NOEs for diastereomer of **20****  
 C5-Et/ C2-H, C10-H $\alpha$ , C4-OBn, C6-H $\alpha$ , C7-H  
 C4-H/ C6-H $\beta$ , C6-H $\beta$ / C19-H $_2$   
 C6-H $\alpha$ / C7-H

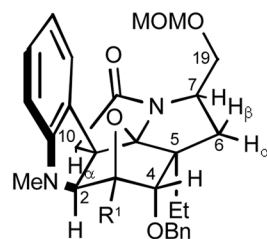
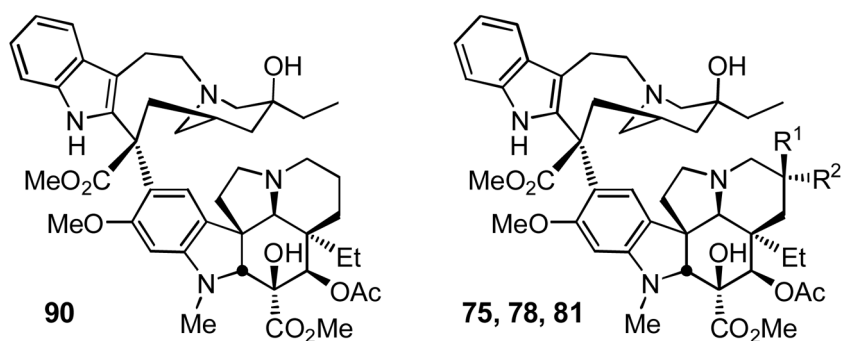
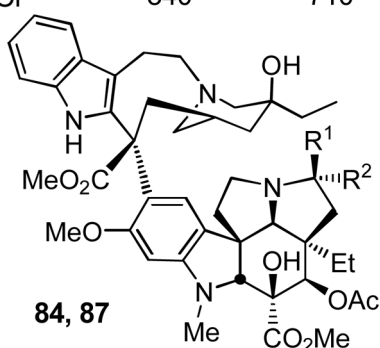


**Figure 3.**  
 Structure of minor diastereomers and diagnostic NOEs.

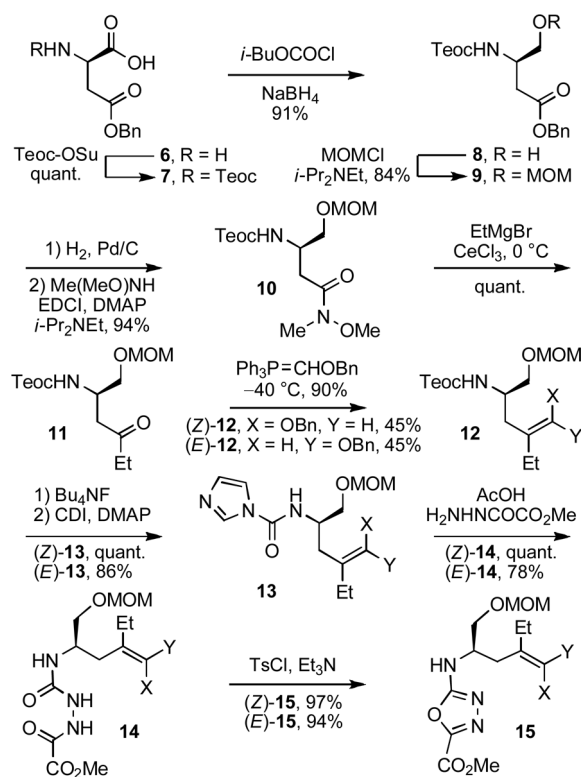


Compound	IC <sub>50</sub> (nM)		
	L1210	HCT116	HCT116/VM46
<b>1</b> , vinblastine	5.6	5.0	600
<b>90</b> , $\Delta^{6,7}$ -dihydrovinblastine	570	370	4500
<b>75</b> , R <sup>1</sup> = OH, R <sup>2</sup> = H	610	630	>10000
<b>78</b> , R <sup>1</sup> = H, R <sup>2</sup> = OH	7600	7700	>10000
<b>81</b> , R <sup>1</sup> = H, R <sup>2</sup> = Cl	840	710	8600

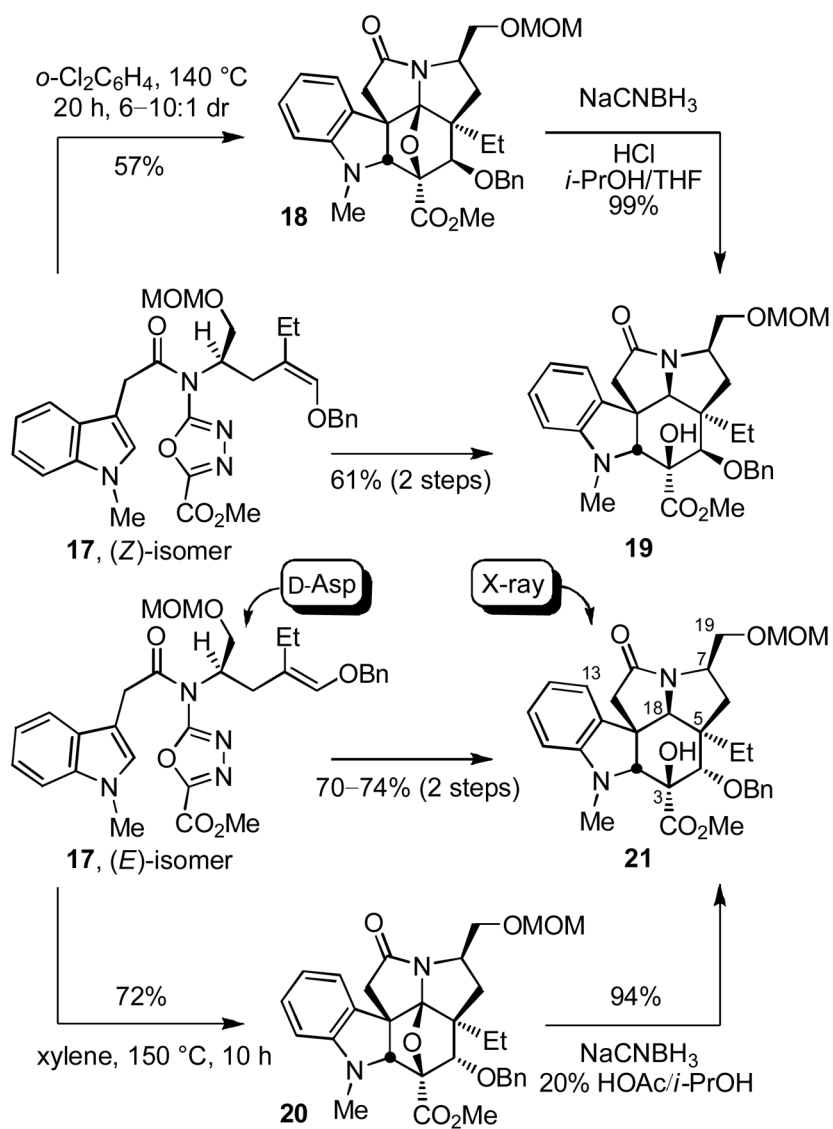


Compound	IC <sub>50</sub> (nM)		
	L1210	HCT116	HCT116/VM46
<b>84</b> , R <sup>1</sup> = CH <sub>2</sub> OH, R <sup>2</sup> = H	4800	870	>10000
<b>87</b> , R <sup>1</sup> = H, R <sup>2</sup> = CH <sub>2</sub> OH	5900	3300	>10000

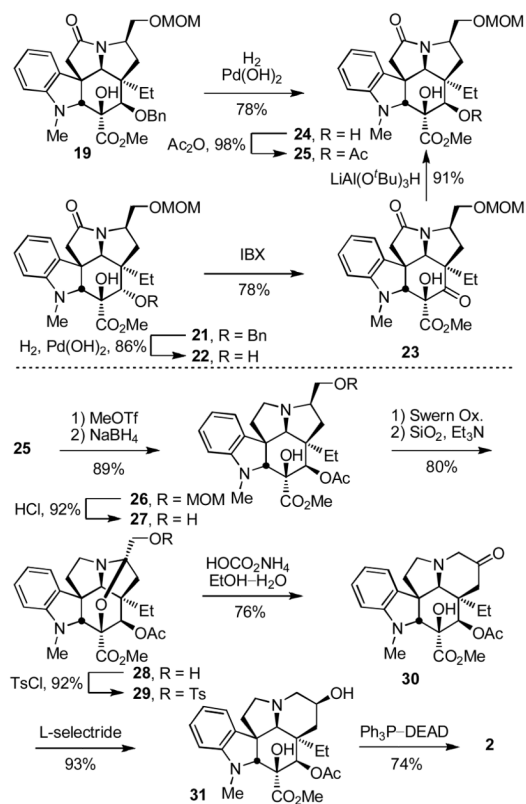
**Figure 4.**  
Cytotoxic activity.



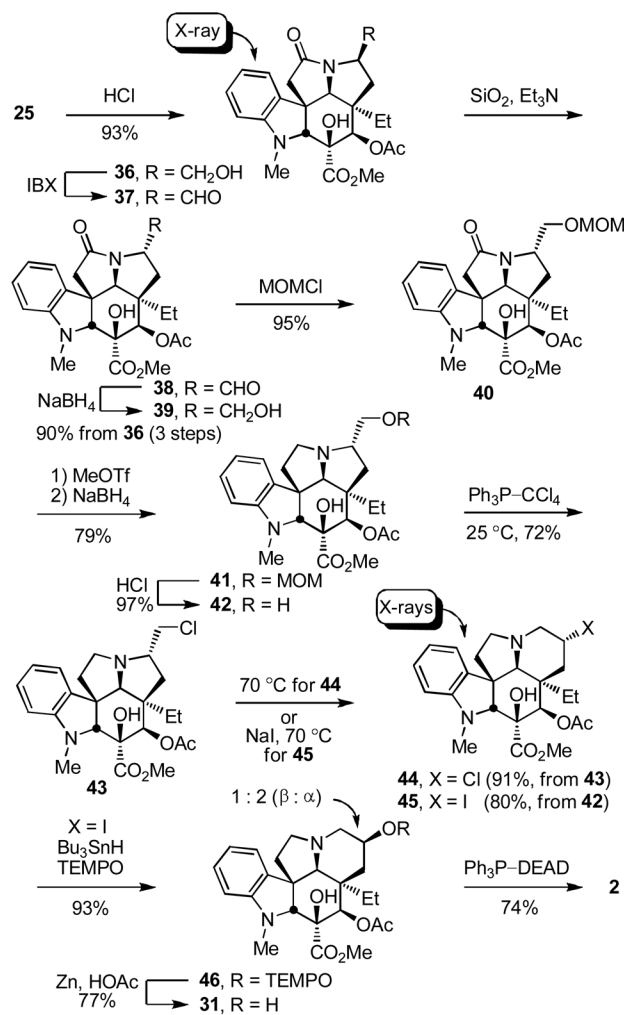
Scheme 1.



Scheme 2.

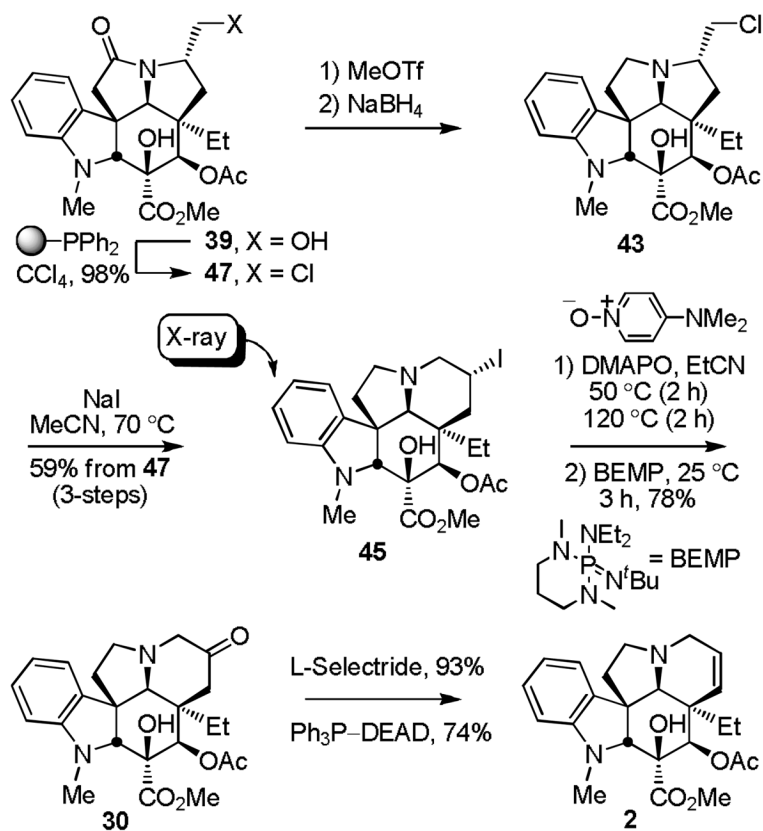


Scheme 3.

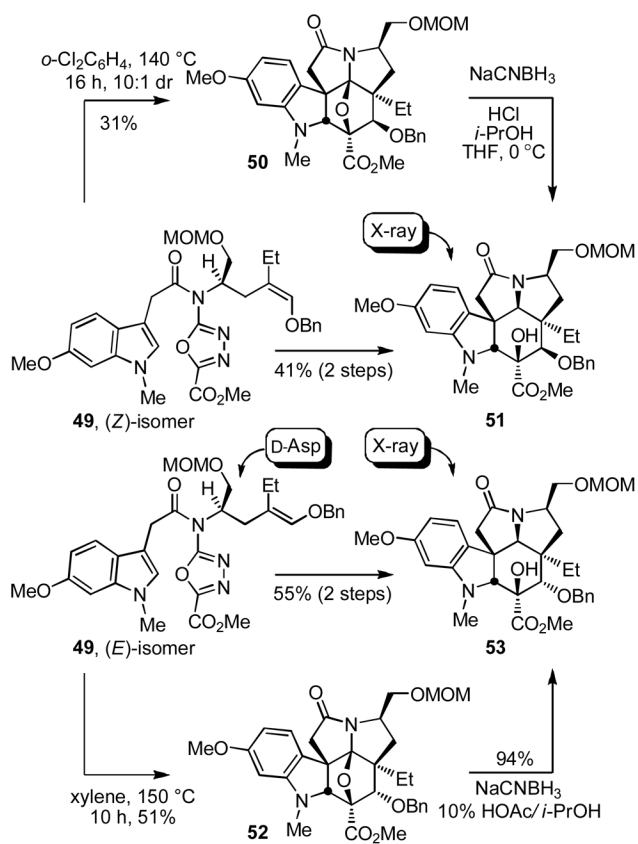


Scheme 4.

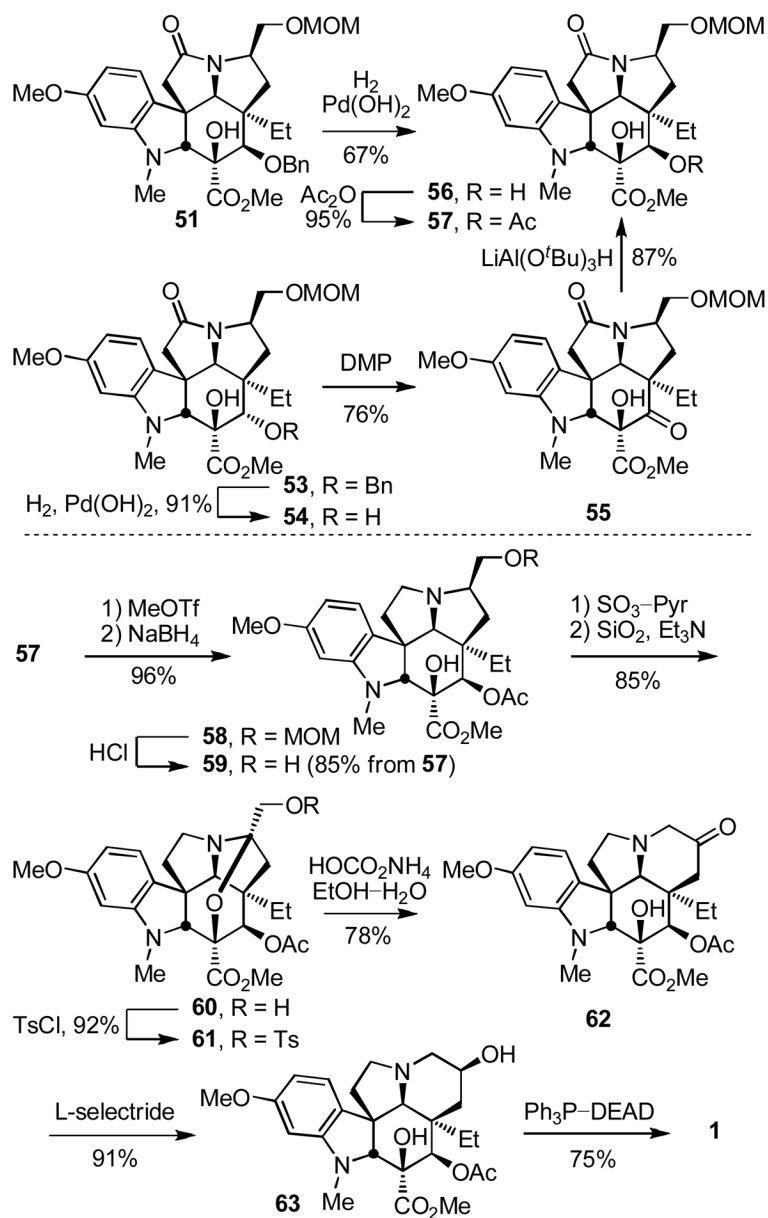




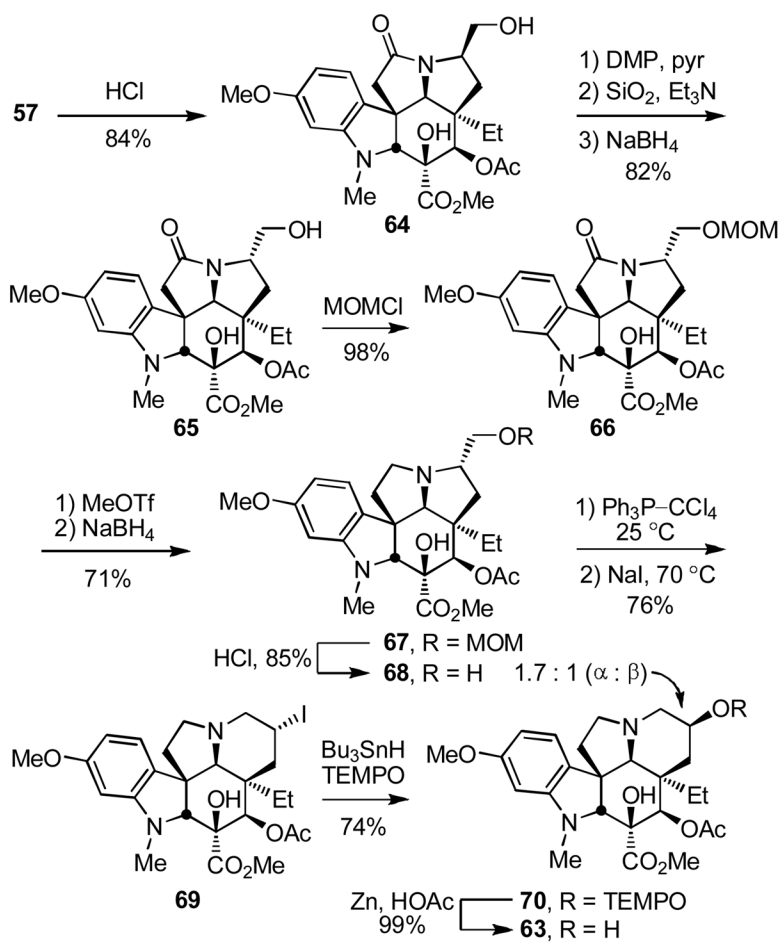
Scheme 5.



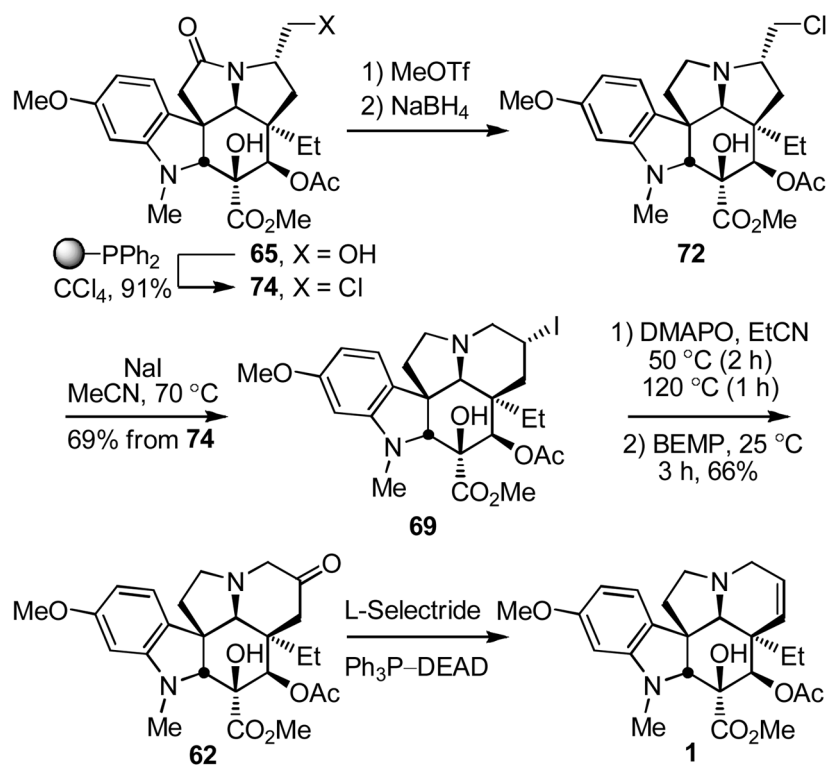
Scheme 6.



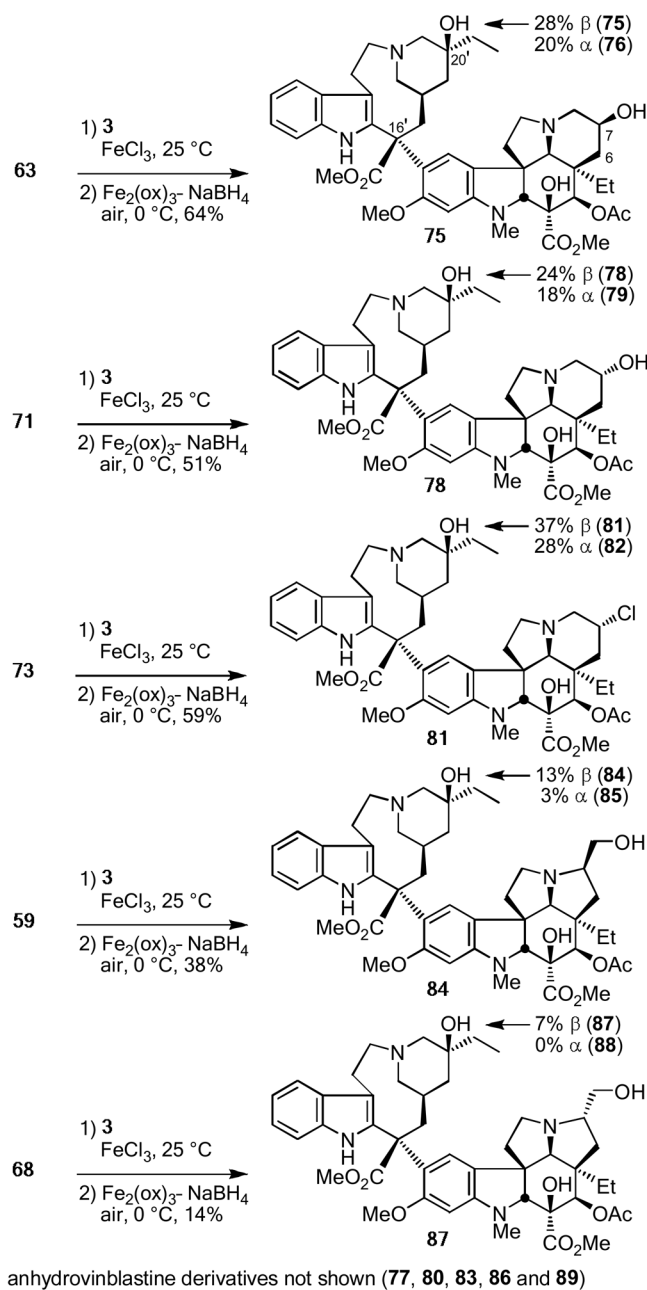
Scheme 7.



Scheme 8.



Scheme 9.



Scheme 10.